PHYSICAL REVIEW B VOLUME 12, NUMBER 8 15 OCTOBER 1975

Study of the optic phonons in the III-V quaternary alloy system: $Ga_{1-x}Al_xAs_{1-y}P_y$ by the average t-matrix approximation

P. N. Sen and G. Lucovsky
Xerox Palo Alto Research Center, Palo Alto, California 94304
(Received 10 March 1975)

The average-t-matrix approximation (ATA) is applied to a study of the ir-active optic phonons in the III-V quaternary alloy system $Ga_{1-x}Al_xAs_{1-y}P_y$. Assignments of the features in the ir reflectance of GaAs-rich and GaP-rich alloys has been previously based on qualitative comparisons with the pseudobinary alloys, $GaAs_{1-x}P_x$ and $Ga_{1-x}Al_xAs$, and the end-member compounds. New results presented in this paper for a $Ga_{1-x}Al_xP$ alloy indicate serious limitations in this approach. To obtain a more quantitative basis for mode assignments in the quaternaries, studies of the optic-phonon density of states have been made using the ATA. Calculations are restricted to linear-chain models with a mass-defect formulation in which changes in the optic-phonon density of states are the result of the mass substitutions. In the low-concentration limit, the ATA is shown to give results that are similar to the coherent-potential approximation. By comparing alloy ϵ_2 spectra with the ATA density of states, it is possible to unambiguously identify all of the features in the ir reflectance spectra. For the dilute alloys considered in this paper, the most interesting features in the spectrum are pair-impurity modes.

I. INTRODUCTION

Lucovsky, Burnham, Alimonda, and Six[1] studied the optic phonons in the quaternary system $Ga_{1-x}Al_xAs_{1-y}P_y$ by infrared (ir) reflectance and assigned the quaternary spectral features by comparisons with the reflectance spectra of appropriate pseudobinaries. For example, they compared a GaAs-rich quaternary with spectra reported in the literature for $GaAs_{1-x}P_x$,[2,3] and $Ga_{1-x}Al_xAs$.[4] In this paper, we report the reflectance spectra for a $Ga_{1-x}Al_xP$ alloy and demonstrate that the assignment of a weak feature at ~ 400 cm^{-1} to a disorder-induced short-wavelength mode in one of the GaP-rich quaternaries is not supported by this new result. This has prompted us to undertake a more complete theoretical analysis of the optic phonons in which the emphasis is on the mode assignments. The body of this paper is related to model calculations of the one-phonon density of states of pseudobinary and quaternary alloys. The model calculations are based on the application of the average-t-matrix approximation (ATA) to linear-diatomic-chain models. These analyses support the assignments of Ref. 1 for the GaAs-rich quaternaries and provide a parallel explanation for the structure in the GaP-rich quaternaries. In particular, the 400-cm^{-1} feature in the GaP-rich quanternaries is assigned to a pair-impurity mode associated with Al-As vibrations in the GaP host.

Section II is a summary of the relevant experimental data. We include the new results on the ir reflectance of $Ga_{1-x}Al_xP$, and then compare the ϵ_2 spectra (ϵ_2 is the imaginary part of the complex dielectric constant ϵ_c) of the quaternaries with the relevant pseudobinaries. Section III deals with model calculations of the phonon-vibrational density of states of pseudobinary and quaternary alloys. It is well established for III-V pseudobinary alloys that mass disorder, rather than force-constant changes, is the dominant factor in determining the character of the optic-mode behavior of the alloys.[5-7] The first-order effects of mass substitutions are readily evident in linear-chain models[8] and have been demonstrated to give results that are applicable to real crystals as well.[7,9] Force-constant changes with composition may, however, be important in determining the variation of mode frequencies with alloy composition.[4] In this section, we first review the single-cell approximations that have been applied to alloy systems; the virtual-crystal approximation (VCA), the coherent-potential approximation (CPA), and the average-t-matrix approximation (ATA). Sen and Hartmann[9] have applied the CPA to diatomic pseudobinary alloys systems using a linear-chain model and have demonstrated that it provides a reasonable basis for understanding the one- or two-mode[5-7] behavior of the optic phonons in real systems. Applications of the ATA have emphasized the electronic energy states of metalic alloys.[10,11] In this paper, we apply the ATA for the first time to the vibrational states of diatomic systems and demonstrate that for dilute pseudobinary alloys it gives results similar to the CPA. Recently, Kamitakahara and Taylor[12] have also studied the vibrational states in simple binary alloys by the ATA. Since the ATA affords economies and conveniences in computation without a sacrifice of physically interesting solutions, it is shown to be a useful tool for studying quaternary systems. Features in the ATA one-phonon density of states are identified by comparisons with calculations of linear-chain single-impurity[8] and pair-impurity modes. The procedure

for obtaining pair-mode frequencies is derived in this paper.

Section IV is devoted to comparisons of the quaternary-alloy spectra with the ATA calculations. We find it convenient to compare the ϵ_2 spectra of the alloys with the ATA density of states. Calculations of the dielectric susceptibility in the ATA are used to confirm the ir activity of the optic modes.

II. EXPERIMENTAL RESULTS

In this section, we review the experimental results on the quaternary system $Ga_{1-x}Al_xAs_{1-y}P_y$, [1] and then make comparisons with pseudo-binary alloy systems. Direct comparisons of infrared reflectance are difficult to interpret since the reflectance R is a complicated function of the oscillator parameters through the dielectric constant ϵ_c;

$$R = \left| (\sqrt{\epsilon_c} - 1)/(\sqrt{\epsilon_c} + 1) \right|^2 \quad . \tag{1}$$

In crystalline solids, including both compounds and their alloys, the optically active phonons are very well approximated by damped harmonic oscillators. The dielectric constant is then constructed as a linear superposition of the contributions of the individual oscillators; i.e.,

$$\epsilon_c = \epsilon_1 - i\epsilon_2 = \epsilon_\infty + \sum_{j=1}^{N} \frac{s_j \nu_j^2}{\nu_j^2 - \nu^2 + i\gamma_j \nu_j \nu} \quad . \tag{2}$$

ϵ_1 and ϵ_2 are, respectively, the real and imaginary parts of the complex dielectric constant; ϵ_∞ is the optical-frequency dielectric constant; ν_j is the oscillator frequency (in cm^{-1}) of the jth mode; s_j is the oscillator strength, and γ_j is a damping parameter; the sum on j is over N phonon modes. The linearity in the sum and the functional form of ϵ_2 make it a natural parameter for comparisons between materials. We consider two of the five samples discussed in Ref. 1. The oscillator parameters for the GaAs-rich sample (No. 154) are taken directly from Ref. 1. The oscillator parameters for the GaP-rich sample (No. 262) are the result of a five-oscillator fit we have undertaken and include a consideration of weak structure near 400 cm^{-1}. In Ref. 1, the spectrum was fitted with four oscillators ignoring the weakest feature. Oscillator parameters for both quaternary-alloy samples are contained in Table I. Before discussing the assignments made in Ref. 1, we present the newly obtained reflectance data for $Ga_{1-x}Al_xP$.

The $Ga_{1-x}Al_xP$ alloy ($x = 0.2$) was grown by liquid phase epitaxial growth on a GaP substrate. The sample was sufficiently thick so that the reflectance, in the region of interest, 250 to 520 cm^{-1}, probed only the $Ga_{1-x}Al_xP$ layer with no interference or other effects associated with the interface or GaP substrate. Figure 1 contains the reflectance spec-

TABLE I. Oscillator parameters used to construct the ϵ_2 spectra of the quaternary and pseudobinary alloys. In using the data of Ref. 2, we did not include the very weak oscillators which make no obvious contribution to the ϵ_2 spectrum. These oscillators were included in Ref. 2 as part of a fit to a particular force-constant model.

Alloy composition	Optical-frequency dielectric constant ϵ_∞	Oscillator frequency ν_j (cm^{-1})	Oscillator strength s_j	Damping constant γ_j	Reference
$Ga_{0.96}Al_{0.04}As_{0.88}P_{0.12}$	10.0	417	0.06	0.04	a
		354	0.48	0.07	
		265	1.92	0.03	
$Ga_{0.92}Al_{0.08}As_{0.16}P_{0.84}$	10.5	434	0.31	0.04	a
		402	0.02	0.02	
		372	0.45	0.03	
		357	1.75	0.02	
		269	0.30	0.05	
$GaAs_{0.94}P_{0.06}$	9.0	356	0.11	0.015	b
		339	0.08	0.045	
		270	1.67	0.015	
$GaP_{0.75}As_{0.25}$	9.65	373	0.31	0.026	b
		361	1.22	0.008	
		272	0.14	0.03	
$Ga_{0.8}Al_{0.2}As$	8.63	358	0.04	0.013	c
		271	1.44	0.020	
$Ga_{0.8}Al_{0.2}P$	9.65	440	0.37	0.028	c
		378	0.50	0.016	
		364	1.24	0.012	

[a]Reference 1. [b]Reference 2. [c]This work.

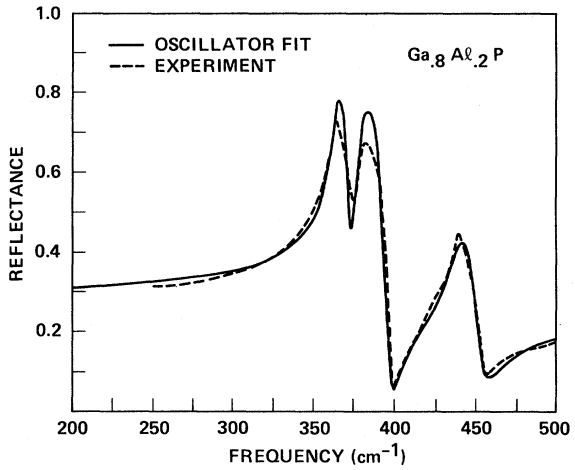

FIG. 1. ir reflectance spectra for $Ga_{0.8}Al_{0.2}P$. The dashed curve is the experimental data; the solid curve is the oscillator fit.

trum; also included in the figure is a spectrum synthesized from oscillator parameters. The oscillator fit was obtained via an iterative search

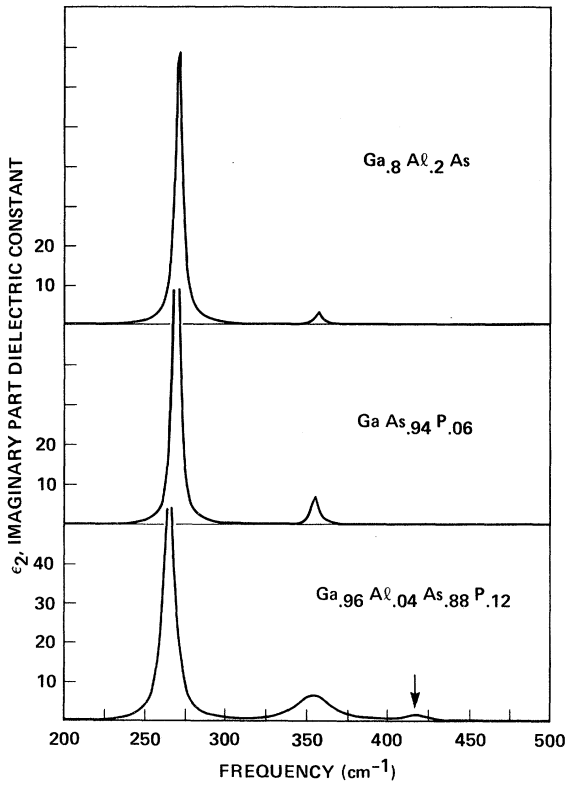

FIG. 2. Comparison of the ϵ_2 spectrum of $Ga_{0.96}Al_{0.04}As_{0.88}P_{0.12}$ with the ϵ_2 spectra of the pseudobinary alloys $GaAs_{0.94}P_{0.06}$ and $Ga_{0.8}Al_{0.2}As$. The arrow identifies the feature in the quaternary not present in either pseudobinary.

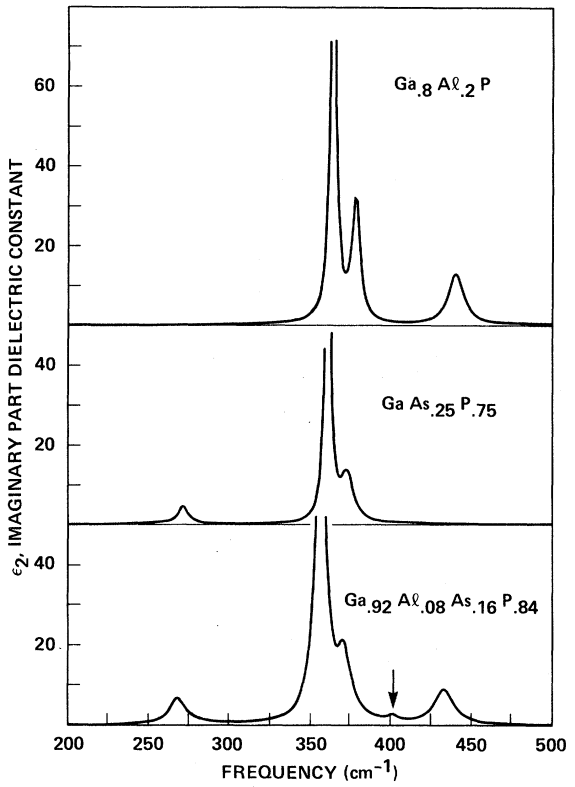

FIG. 3. Comparison of the ϵ_2 spectrum of $Ga_{0.92}Al_{0.08}As_{0.16}P_{0.84}$ with the ϵ_2 spectra of the pseudobinary alloys $GaAs_{0.25}P_{0.75}$ and $Ga_{0.8}Al_{0.2}P$. The arrow identifies the feature in the quaternary not present in either pseudobinary.

in a multiparameter space in which the experimental reflectance is compared to a reflectance synthesized from three damped harmonic oscillators via Eqs. (1) and (2).

Figures 2 and 3 contain comparisons of the ϵ_2, spectra of the quaternaries with the relevant pseudobinaries. In Fig. 2, the GaAs-rich quaternary is compared with two GaAs-rich alloys: $GaAs_{0.94}P_{0.06}$,[2] and $Ga_{0.90}Al_{0.10}As$.[4] In Fig. 3, the ϵ_2 spectrum of the GaP-rich quaternary is compared with the ϵ_2 spectra of two alloys: $GaAs_{0.25}P_{0.75}$,[2] and $Ga_{0.8}Al_{0.2}P$. The oscillator parameters for the $Ga_{0.8}Al_{0.2}P$ sample are those obtained in this study.

Consider first the GaAs-rich system. The assignments made in Ref. 1 are entirely supported by the comparisons given in Fig. 2 and by our calculations as well. The peak at 260 cm^{-1}, dominant in all three alloys, is clearly due to Ga-As vibrations of the host crystal. The broad peak near 360 cm^{-1} in the quaternary overlaps the local-mode features that occur in *both* the $GaAs_{1-x}P_x$ and $Ga_{1-x}Al_xAs$ as alloys supporting the assignment of this feature of *both* Ga-P and Al-As vibrations.

Finally, there is no feature in either ternary near 420 cm^{-1}, whereas there is a feature in the quaternary alloy. The frequency and relative strength of this feature in the quaternary suggest that it is due to Al-P pair vibrations in the GaAs host.[1]

Consider next the GaP-rich quaternary alloy. The assignments of Ref. 1 were predicted on an assumption that the vibrational frequency for Al-As vibrations in a GaP host was degenerate with the GaP-host reststrahlen. This assumption was based on the near equality of the [2,3] GaP and[4] AlAs reststrahlen bands and did not take into account the difference in the neighborhood of an Al-As pair in a GaP host and an AlAs host. As we demonstrate later in this paper, these differences in the local environment have a strong effect on the pair-mode frequency. With this assumption of degeneracy and the obvious assignments of the 260 cm^{-1} feature to Ga-As vibrations, and the 430 cm^{-1} feature to Al-P vibrations, the features at 370 and 400 cm^{-1} were assigned to disorder-induced short-wavelength modes. The assignment of the 370 cm^{-1} feature is well established by studies on other alloy systems, $GaAs_{1-x}P_x$ (Ref. 13) and $In_{1-x}Ga_xP$ (Ref. 14), as well as neutron studies on pure GaP (Ref. 15). Since the 400-cm^{-1} feature did not occur in the $GaAs_{1-x}P_x$ system,[2,3] it was assumed to be related to Al-P vibrations. The spectrum we show in this paper for $Ga_{0.8}Al_{0.2}P$ does not support this assignment nor do studies that have been made on other alloys in the $Ga_{1-x}Al_xP$ system.[16] The model calculations that we have performed and describe in Sec. III demonstrate that the 400-cm^{-1} feature in the GaP-rich quaternary is due to an Al-As pair mode in the GaP host. Our calculations support the other assignments of Ref. 1, relating to the frequencies of Ga-P, Ga-As, and Al-P modes.

III. THEORY

A. Single-cell approximations

In this section, we review the single-cell approximations that have been applied to alloy systems. There are three mean-field approximations to consider, the virtual-crystal approximation (VCA), the coherent-potential approximation (CPA), and the average-t-matrix approximation (ATA). The CPA has been applied to the lattice-dynamical problem by Sen and Hartmann[9] and others[17,18] and has proved to be a useful approach. The ATA has been applied mostly to the electronic density of states of metallic alloys,[10,11] where Schwartz *et al.*[10] have demonstrated that for dilute binary alloys it gives results similar to the CPA. The ATA has also recently been used to study the vibrational states in binary alloys.[12]

We now develop the lattice-dynamical equations of motion for alloy systems and indicate how the CPA and ATA can be applied. For our model calculations, we assume that there are no force-constant changes on alloying. This means that the dynamical matrix, which we denote by $D_{ll'}^{\alpha\beta}$, remains unchanged over the entire composition. The equation of motion for the αth atom in the lth sublattice is given by

$$M_{l\alpha}\omega^2 u_{l\alpha} = \sum_{l'\beta} D_{ll'}^{\alpha\beta} u_{l'\beta}, \tag{3}$$

where $u_{l\alpha}$ denotes the displacement. The Green's function $G(\omega^2)$ is defined in the usual manner and is a function of ω^2, the frequency squared.

In an alloy, $M_{l\alpha}$ is random. Let G^0 be the Green's function for the perfect crystal, and let M_0 be the corresponding mass matrix. For the purposes of the single-cell approximation, one introduces a reference medium characterized by a cell-independent self-energy matrix $\sigma(\omega^2)$. σ is diagonal in the lattice index l and is an $(nr)\times(nr)$ matrix, where r is the number of atoms in a cell and n the dimension of the lattice. Explicitly,

$$\sigma_{ll'}^{\alpha\beta} = \sigma^{\alpha\beta}\delta_{ll'}. \tag{4}$$

The reference Green's function $\tilde{G}$ is given by

$$\tilde{G} = G^0 + G^0\sigma\tilde{G}. \tag{5}$$

In an alloy, each cell possesses a random deviation from σ, and one can define a t matrix for the lth cell associated with this deviation; i.e.,

$$t_l = \{1 - [(M_0 - M_l)\omega^2 - \sigma]\tilde{F}(\omega^2)\}^{-1}[(M_0 - M_l)\omega^2 - \sigma], \tag{6}$$

where

$$\tilde{F} = \tilde{G}_{ll} = \frac{1}{N}\sum_{\vec{k}} \tilde{G}(\vec{k}). \tag{7}$$

If one further defines a cell-independent self-energy matrix Σ which relates $\bar{G}$ to G^0 through

$$\bar{G} = G^0 + G^0\Sigma\bar{G}, \tag{8}$$

then it can be shown, in the single-cell approximation, that

$$\Sigma = \sigma + (1 + \langle t_n\rangle\tilde{F})^{-1}\langle t_n\rangle, \tag{9}$$

where $\langle\ \rangle$ denotes an average over the alloy configuration. The various mean-field approximations can then be characterized in terms of Eq. (9). In the VCA, one assumes that all the cells are represented by average masses and neglects the terms involving $\langle t\rangle$, so that

$$\sigma_{\alpha\beta} = (M_0 - \bar{M})_\alpha\omega^2\delta_{\alpha\beta} = \Sigma_{\mathrm{VCA}}. \tag{10}$$

The VCA always yields a one-mode behavior for the optic phonons. In the ATA, one assumes a trial σ, and using (6) and (9), obtains a value for Σ. This calculation for Σ can be improved iteratively by using the calculated Σ as the new input

for σ. In this way, the ATA attributes to each cell an average scattering strength. For the numerical studies in this paper, we use the VCA to determine a value for σ and then use Eqs. (6) and (9) to define Σ; we do not attempt to improve Σ through an iterative procedure. The CPA, which is believed to be the best single-cell approximation of these three,[11] attempts to evaluate the reference-crystal self-energy σ in a self-consistent way, by requiring that $\langle t_n \rangle = 0$, so that $\Sigma = \sigma$. This implies that the self-consistent reference medium is such that there is no further scattering due to deviations at each cell.

The density of states and the lattice susceptibility are given by a conditional configuration average, discussed in detail in Ref. 9;

$$\rho(\omega^2) = -\frac{1}{\pi N} \operatorname{Im} \operatorname{Tr} \langle \mathrm{MG} \rangle , \tag{11}$$

$$\chi(\omega^2) = \frac{1}{N^2} \sum_{l\alpha} \sum_{l'\beta} \langle Q_{l\alpha} Q_{l'\beta} G_{ll'}^{\alpha\beta} \rangle . \tag{12}$$

$Q_{l\alpha}$ denotes the charge on the αth atom in lth lattice. The conditional configuration averaging is straightforward, but the algebra is involved and we will not give details here. The density of states integrated over the entire spectrum remains constant in alloying, since it is a measure of the total number of degrees of freedom in the system.

In this paper, we consider pseudobinary and quaternary alloys which have only two sublattices. We will assume that charges on the two sublattices are equal to Q and $-Q$, respectively, and are independent of the kind of atom. This is a reasonable approximation for binary compounds and their alloys, particularly the III-V's, and serves to simplify the expression for χ,

$$\chi = Q^2 [\bar{G}^{11} + \bar{G}^{22} - (\bar{G}^{12} + \bar{G}^{21})]_{\vec{k}=0} . \tag{13}$$

The virtue of the ATA from computational point of view is that the ATA is straightforward. To implement the CPA, one has to solve a complicated matrix equation to determine Σ. For ATA this is not necessary. Secondly, for the ATA, χ is obtained almost trivially in terms of the G_{ll}^0 and Σ, since one needs only the value of the Green's function matrix at $\vec{k} = 0$. For the CPA, however, one has to perform the k sum on $\bar{G}$ to solve for Σ. Since Σ is a matrix, this is often a tedious calculation, even for those cases in which G_{ll}^0 may be simply evaluated.

B. One-dimensional diatomic chain

In this section of the paper, we apply the CPA and ATA to the lattice dynamics of linear-diatomic chains. The classic work of Mazur, Montroll, and Potts[8] has established the power of such a simple model, in particular, in elucidating the types of phonon behavior which can occur in monatomic and diatomic systems. Linear-chain models traditionally give more optic modes than are observed in real systems. Lucovsky *et al.*[7] have developed a procedure that systematically eliminates "spurious" local modes and shows very good quantitative agreement with real systems. The work of Mazur, Montroll, and Potts[8] was restricted to single impurities in otherwise perfect chains. Alloy linear chains have also been considered extensively by Dean and co-workers[19] and by Sen and Hartmann.[9] In this paper, we review briefly the application of the CPA to pseudobinary alloys and then indicate how the ATA is applied to these same systems and compare the results. Finally, we consider the application of the ATA to quaternary systems.

We first consider a perfect diatomic chain in which the masses of the atoms on the two sublattices are labeled M_1 and M_2, respectively. We consider only nearest-neighbor harmonic forces. If f is the force constant, then the zone-boundary frequencies ω_1 and ω_2 are given by

$$\begin{aligned} \omega_1^2 &= 2f/M_1 , \\ \omega_2^2 &= 2f/M_2 . \end{aligned} \tag{14}$$

The optic-mode frequency at Γ, ω_T, is then given by

$$\omega_T^2 = \omega_1^2 + \omega_2^2 . \tag{15}$$

It is convenient to characterize substitutional defects on sublattices 1 and 2 by mass-defect parameters $\bar{\epsilon}_1$ and $\bar{\epsilon}_2$, respectively:

$$\bar{\epsilon}_j = \left(1 - \frac{M_j'}{M_j}\right), \qquad j = 1, 2 , \tag{16}$$

where M_j' is the mass of the substitutional atom on the jth sublattice. We define the respective impurity concentrations by x and y. For the case of a pseudobinary, $\bar{\epsilon}_2 \equiv 0$ and y is therefore a redundant parameter. In Sec. IV we discuss the application of the CPA and ATA to pseudobinary alloys.

C. Pseudobinary alloys: CPA and ATA

A detailed treatment of the CPA as applied to the lattice dynamics of pseudobinary alloys in linear chains can be found in (Ref. 9). In this section we emphasize the application of the ATA to the same type of alloy systems. In the ATA, one finds by conditional configurational averaging that

$$\rho(\omega^2) = -\frac{1}{\pi} \operatorname{Im} \left[\left(M_1 - \frac{\Sigma}{\omega^2} \right) \bar{G}_{ll}^{11} + M_2 \bar{G}_{ll}^{22} \right]. \tag{17}$$

Before we compare numerical results for the CPA and ATA, we demonstrate that for very small concentrations, the ATA and CPA give similar results for the self-energy and hence the density of states. This has already been demonstrated for the elec-

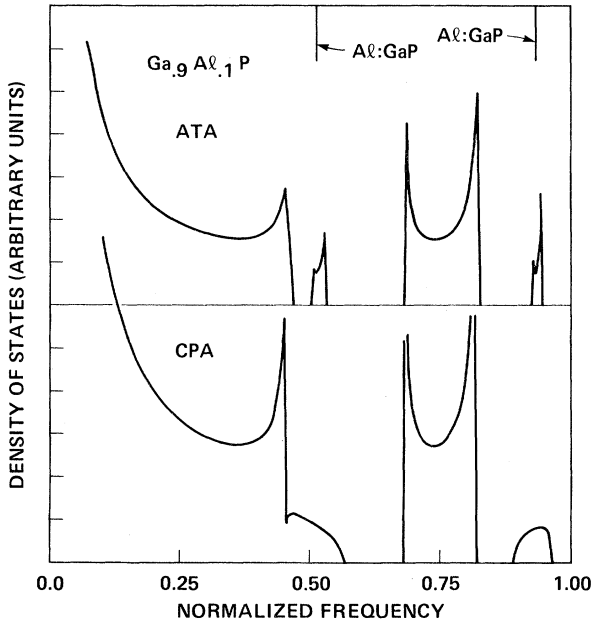

FIG. 4. Comparison of the CPA and ATA density of vibrational states for the alloy $Ga_{0.9}Al_{0.1}P$. Also indicated are the frequencies of the two Al-impurity modes in Gap. The higher-frequency mode is ir active, whereas the lower-frequency mode is not.

tronic energy states[10]; we now demonstrate a similar result for the vibrational density of states associated with linear chains. The self-energy Σ in the CPA is given by

$$\Sigma_{\mathrm{CPA}} = \frac{x\bar{\epsilon}_1 M_1\omega^2}{1+(\Sigma_{\mathrm{CPA}}-\bar{\epsilon}_1 M_1\omega^2)\bar{F}^{11}} \cdot \tag{18}$$

The self-energy in the ATA it is given by

$$\Sigma_{\mathrm{ATA}} = x\bar{\epsilon}_1 M_1\omega^2 + \frac{x(1-x)\bar{\epsilon}_1^2 M_1^2\omega^4\tilde{F}^{11}}{1-(1-2x)\bar{\epsilon}_1 M_1\omega^2\bar{F}^{11}} \cdot \tag{19}$$

In the limit of small concentrations $x \sim 0$, these two expressions become identical. Kamitakahara and Taylor[12] also found that in a system with one atom per unit cell, the ATA and CPA gave similar results for low concentrations. This result is valid for the general case of any dimentionality.

We are now ready to make comparisons between the ATA and CPA vibrational densities of states for pseudobinaries. We restrict our discussion to a specific example to illustrate the salient points. If we consider a single Al impurity in an infinite GaP chain, then we expect both a gap and a local mode[8]; the local mode "rises" out of the top of the optic branch and is ir active, whereas the gap mode has its "parentage" in the acoustic branch and is not ir active. The local mode is observable in real systems[4] and the mass defect associated with the Al for Ga substitution, 0.61, exceeds the critical value of 0.46 given by Lucovsky *et al.*[7] In Fig. 4, we compare the CPA and ATA densities of states for $x = 0.1$. Also included are the positions of the local- and gap-mode frequencies as computed from the linear-chain model of Mazur, Montrol, and Potts.[8] There are several points to be made: (i) The frequencies of the local and gap modes in the CPA, ATA, and single-impurity calculations are all comparable. For the alloy case, we consider $x = 0.1$, the local and gap modes have developed into bands. (ii) The impurity bands in the ATA are sharper than those obtained using the CPA. Since the CPA bands are very similar to those calculated by Dean *et al.*[19] we take this comparison to indicate that the ATA underestimates damping and hence produces sharper impurity bands. The impurity band width given by the CPA is about three times that of the ATA. This result for vibrational modes is essentially similar to that obtained for the electronic states in binary metallic alloys.[10] Note also that in the ATA, the gap mode is completely split from the acoustic branch of the host, whereas in the CPA they are merged. However, this example should not be taken to imply that impurity modes are always split off in the ATA, even in one-dimensional chains. We have made detailed numerical investigations and found that depending on the relative masses, one can also obtain situations where the ATA impurity band is merged with the parent band of the host.

D. Quaternary alloys

In this section we extend our calculations to quaternary alloys of the general composition $A_{1-x}B_xC_{1-y}D_y$, where AC is the "host" lattice and B and D are "impurities," respectively, on sublattices 1 and 2. For the ATA, one has to interchange the role of impurity and host atoms for x or $y > 0.5$, whereas in the CPA this distinction is unnecessary. In what follows we restrict our calculations to the ATA. Since it is a single-cell approximation, it is necessary to consider the various nearest-neighbor configurations that are possible in the quaternary; these are AC, AD, BC, and BD and occur with relative probabilities of $(1-x)(1-y)$, $(1-x)y$, $x(1-y)$, and xy, respectively. For each configuration, we can define in a straightforward way 2×2 matrices [see Eq. (6)] and combining these we obtain a self-energy, given by Eq. (9), when the average of the t matrices is weighted approximately.

Figures 5 and 6 are the one-phonon densities of states calculated for model GaAs- and GaP-rich quaternaries. In each example we consider the alloy to be 0.90 host and 0.1 of each impurity, i.e., we consider $Ga_{0.9}Al_{0.1}As_{0.9}P_{0.1}$ and $Ga_{0.9}Al_{0.1}As_{0.1}P_{0.9}$.

We include in Figs. 5 and 6 comparisons with the appropriate pseudobinaries. For the GaAs-rich alloy, we include the ATA density of states for

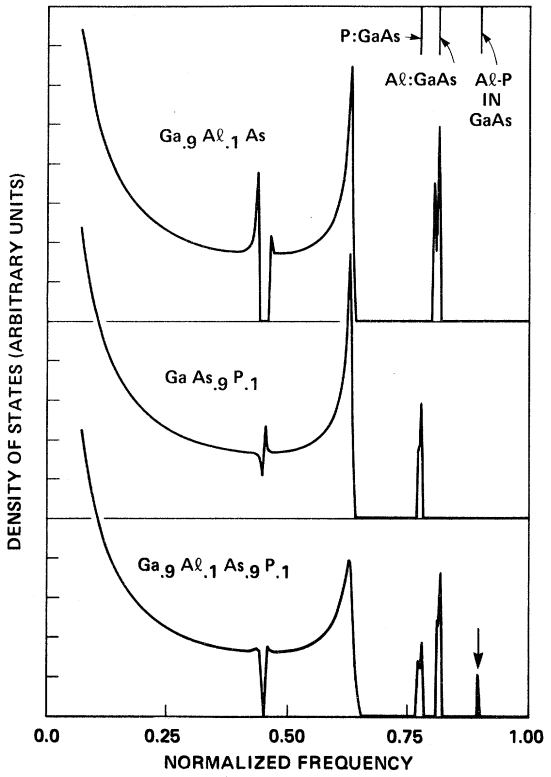

FIG. 5. Comparison of the ATA density of vibrational states for the quaternary alloy $Ga_{0.9}Al_{0.1}As_{0.9}P_{0.1}$ with the ATA densities of states for the pseudobinary systems $GaAs_{0.9}P_{0.1}$ and $Ga_{0.9}Al_{0.1}As$. Also indicated are the impurity and pair-mode frequencies relevant to the quaternary system. The arrow identifies the feature in the quaternary density of states not found in either pseudobinary alloy.

$Ga_{0.9}Al_{0.1}As$ and $GaAs_{0.9}P_{0.1}$; for the GaP-rich alloy, we include $Ga_{0.9}Al_{0.1}P$ and $GaAs_{0.1}P_{0.9}$. Note that in each case *all* but *one* of the quaternary features are identified through these comparisons. The calculation that we now undertake demonstrates that in *each* case the additional quaternary ATA feature is indeed due to a mode associated with a pair of impurity atoms.

Mazur, Montroll, and Potts[8] have considered in detail the effects of single impurities in an otherwise perfect diatomic chain. We now consider the problem of a pair of impurities in an otherwise perfect chain. Let M_1 and M_2 be the masses of the perfect system; let M_1' and M_2' be the masses of the impurity atoms on adjacent sides in sublattices 1 and 2, respectively. Let us label the site by l. We define a mass-defect matrix ϵ_{pq} by

$$\bar{\epsilon}_{pq} = \begin{pmatrix} \bar{\epsilon}_1 & 0 \\ 0 & \bar{\epsilon}_2 \end{pmatrix} \delta_{lp}\delta_{ql} . \tag{20}$$

The Green's function G for the defective lattice is then given by

$$G = G^0 + G^0 \bar{\epsilon} M\omega^2 G , \tag{21}$$

so that the impurity modes are given by

$$\det\left| 1 - \bar{\epsilon} M\omega^2 G^0 \right| = \Delta_R + i\Delta_I = 0 . \tag{22}$$

This equation gives the well-known results of Ref. 8 if either $M_1' = M_1$ or $M_2' = M_2$. If both Δ_R and Δ_I are zero, we obtain a true bound state; however, if $\Delta_R = 0$ but $\Delta_I \neq 0$, we obtain a resonance. Also note that these resonance modes cannot be obtained for single impurities in a diatomic chain and are therefore a new feature of the pair-mode problem. Equation (22) yields a complicated solution for defect modes which is more easily studied numerically than analytically. We have considered a GaAs host with an Al-P impurity pair, and a GaP host with an Al-As impurity pair. Each of these pair-mode calculations yields a single bound state at frequencies in excess of the highest-host-optic mode. For both calculations the frequencies of the pair modes coincide with the extra features in the appropriate ATA quaternary density of states. These calculated frequencies are also indicated in Figs. 5 and 6. The criterion in Ref. 7 suggests

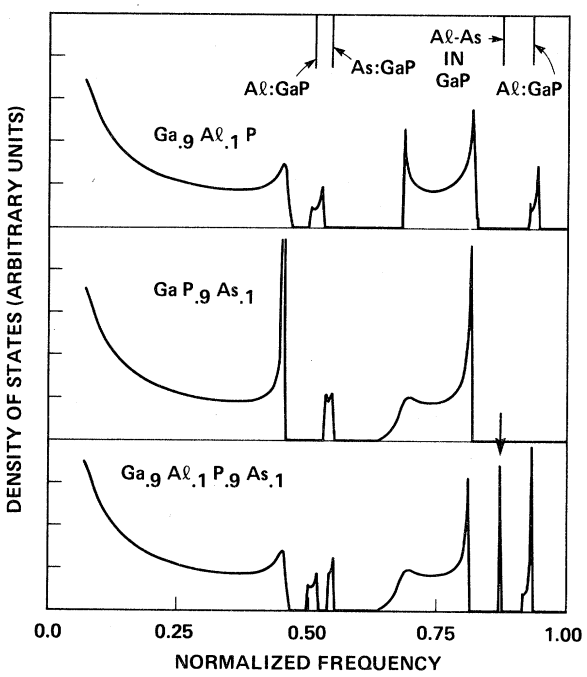

FIG. 6. Comparison of the ATA density of vibrational states for the quaternary alloy $Ga_{0.9}Al_{0.1}P_{0.9}Al_{0.1}$ with the ATA densities of states for the pseudobinary systems $GaP_{0.9}As_{0.1}$ and $Ga_{0.9}Al_{0.1}P$. Also indicated are the impurity and pair-mode frequencies relevant to the quaternary system. The arrow identifies the feature in the quaternary density of states not found in either pseudobinary alloy.

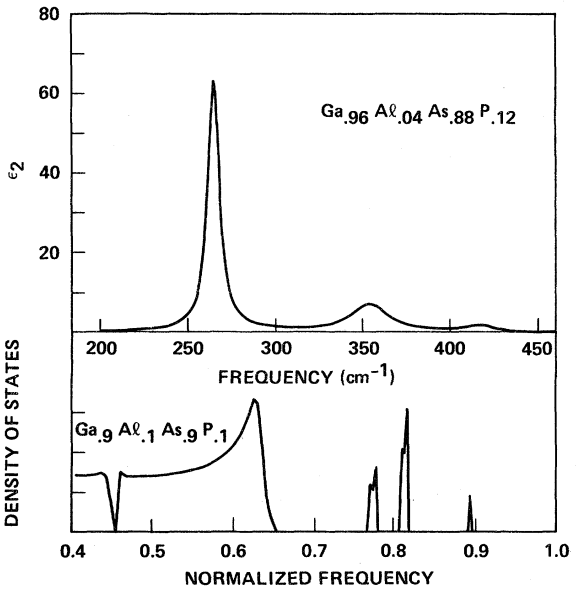

FIG. 7. Comparison of the ϵ_2 spectrum of $Ga_{0.96}Al_{0.04}As_{0.88}P_{0.12}$ with the ATA density of states for $Ga_{0.9}Al_{0.1}As_{0.9}P_{0.1}$.

that in each case the pair-mode frequency is sufficiently high to assure its observability in a real crystal.

There is one other aspect of the pair-mode calculation that is worth noting. This concerns the actual pair-mode frequency. Since we are not considering force-constant changes, one might *a priori* expect the pair-mode frequency of an Al-As pair in a GaP host to be degenerate with the host-optic-mode frequency. This expectation is based on the nearly equal reduced masses of AlAs and GaP and is supported by the near equality of the AlAs and GaP reststrahlen frequencies.[2-4] How then, does one explain the higher frequency of the pair-mode relative to the top of the host GaP optic band? The answer is related to the fact that local modes, whether they be associated with single or pair impurities, involve atomic motions of the host crystal atoms as well as the impurity atom (or atoms).[8] Since the Al atom is substituted on to the Ga sublattice, and the As atom into the P sublattice, the local order in the vicinity of the Al-As pair can be represented by the following linear array of atoms: P-Ga-P-Al-As-Ga-P-Ga. In the local pair-mode motion, the Al and Ga atoms move in phase opposition to the As and P atoms with amplitudes that drop off exponentially with respect to the distance from the impurity site.[8] To a first approximation, one would then expect a pair-mode frequency ω_p to be given by

$$\omega_p \approx \sqrt{\omega_{\mathrm{AlP}}\omega_{\mathrm{AlAs}}}\,, \tag{23}$$

where ω_{AlP} and ω_{AlAs} are, respectively, characteristic frequencies for AlP and AlAs, e.g., the TO-phonon frequencies. In this approximation, $\omega_p \approx 398\ \mathrm{cm}^{-1}$ very close to the calculated frequency. The approximation in Eq. (23) is based on the fact that Al is substantially lighter than As and hence its motion should dominate in an optic mode. A similar effect occurs for GaP vibrations in GaP, GaAs, and GaSb hosts where the respective frequencies decrease from 365 cm^{-1},[6] to 351 cm^{-1},[6] to 324 cm^{-1}.[6]

It now remains to compare the quaternary densities of states to experiment. We make these comparisons using the ϵ_2 spectra of the quaternary alloys and the ATA densities of states. We could have equally well compared the experimental ϵ_2 with calculated susceptibilities as both comparisons lead to the same conclusions regarding the mode assignments.

IV. APPLICATION OF THE ATA TO QUATERNARY ALLOYS

Figures 7 and 8 compare the experimentally derived ϵ_2 spectra for the quaternary alloys with the ATA one-phonon density of states. These comparisons provide a basis for assigning the features in the quaternary ir reflectance to vibrational modes involving specific nearest-neighbor atom-pairs. Figure 7 compares the ϵ_2 spectrum of $Ga_{0.96}Al_{0.04}As_{0.88}P_{0.12}$ with the ATA density of states for $Ga_{0.9}Al_{0.1}As_{0.9}P_{0.1}$. Consider first the ATA density of states. The broad feature extending from ~0.45 to 0.65 (normalized frequency) is due to the optic branch of the host crystal, GaAs. The

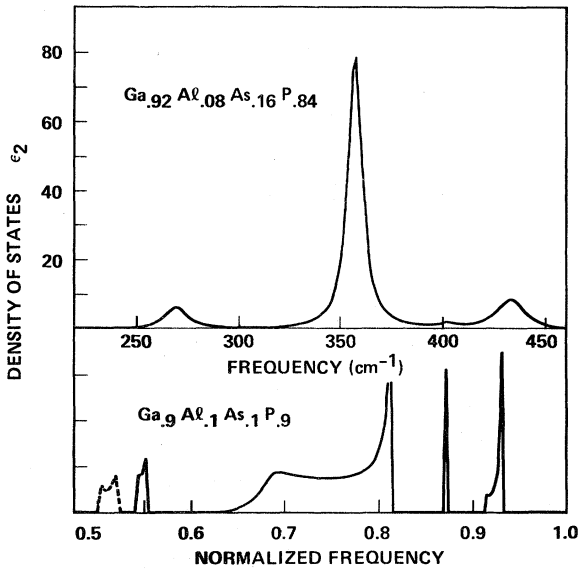

FIG. 8. Comparison of the ϵ_2 spectrum of $Ga_{0.92}Al_{0.08}As_{0.16}P_{0.84}$ with the ATA density of states for $Ga_{0.9}Al_{0.1}As_{0.1}P_{0.9}$.

sharper features are essentially impurity modes, in this example, local modes higher in frequency than the optic modes of the host. All of these modes are optically active in this model as determined from the calculated susceptibility. The features at ~ 0.77 and ~ 0.83 are due to single-impurity modes involving, respectively, Ga-P and Al-As nearest-neighbor pairs. The very sharp and clearly weaker feature at ~ 0.89 is due to Al-P pairs in the GaAs host. A comparison of the ϵ_2 spectrum of the quaternary with the ATA density of states supports the assignments of Ref. 1, namely, that the dominant feature at ~ 265 cm^{-1} is a mode of the GaAs host, the broad feature at ~ 355 cm^{-1} is associated with both Ga-P and Al-As vibrations, whereas the very weak feature at ~ 417 cm^{-1} is due to pairs of impurities Al and P in the GaAs host. If the quaternary under study is assumed to be a true solid solution, then the Al and Ga atoms are randomly distributed on one sublattice, and the As and P atoms on the other. The ATA density of states was calculated subject to this assumption. It was noted in Ref. 1, that the oscillator strengths of the quaternary modes supported a random-bonding model for the alloy. The comparison we make here in Fig. 7 also supports this alloy model.

In Fig. 8 we consider the GaP-rich alloy $Ga_{0.92}Al_{0.08}As_{0.16}P_{0.84}$; we compare the ϵ_2 spectrum of the quaternary with the ATA density of states for $Ga_{0.9}Al_{0.1}As_{0.1}P_{0.9}$. We have not included the contribution of the 370-cm^{-1} mode to the ϵ_2 spectrum. This mode is due to disorder-induced short-wavelength vibrations of the GaP host and is found in pseudobinary as well as quaternary alloys. Consider first the ATA density of states. The broad feature from ~ 0.65 to 0.85 is the optic-phonon branch of the GaP host; the remaining features are impurity modes. The features at ~ 0.5 and 0.92 are due to Al-P vibrations; a calculation of the susceptibility indicates ir activity only in the 0.92 feature. The structure at ~ 0.55 is due to Ga-As vibrations, and finally, the very sharp feature at ~ 0.87 is due to Al-As vibrations in the GaP host. The comparison in Fig. 8 supports three of the assignments of Ref. 1; (i) the 360-cm^{-1} feature is due to the GaP host; (ii) the 260-cm^{-1} feature is due to Ga-As vibrations, essentially gap modes; and (iii) the 435-cm^{-1} feature is due to Al-P vibrations, essentially local modes. Finally, the ATA density of states identifies the very weak 400-cm^{-1} feature in the ϵ_2- spectrum with Al-As vibrations in the GaP host. This assignment is further supported by two other observations: (i) The 400-cm^{-1} feature occurs in all three quaternary alloys reported in Ref. 1, but not in the spectra of the $GaAs_{1-x}P_x$ or $Ga_{1-x}Al_xP$ pseudobinaries[2,3,16]; (ii) The oscillator strength of this mode is consistent with that expected for a random alloy, i.e., the oscillator strength of this pair mode should be proportional to $x(1-y)$, as compared to either the host GaP mode $(1-x)y$, or the Ga-As or Al-P single-impurity modes $(1-x)(1-y)$ and xy, respectively. These relative strengths are supported by the oscillator parameters given in Table I.

V. SUMMARY

We have demonstrated how model density-of-state calculations can be used to assign the features in quaternary-alloy ir reflectance spectra. In particular, we have applied the ATA to diatomic-linear chains and have calculated the changes in the one-phonon density of states associated with mass substitutions. This approach is particularly well suited to the III-V semiconductors for which it is well established that the first-order changes in the phonon spectra are due to mass defects rather than changes in the force constants.

There are many interesting problems remaining to be studied in quaternary alloys. We have explored only a very small portion of one system. We have identified a three-mode behavior for the GaAs-rich alloy and a four-mode behavior for the GaP-rich alloy. We anticipate that other quaternary-alloy systems will display markedly different behaviors related, for example, to different combinations of masses or to changes in force constants that may become important in other types of systems. In general, a diatomic-quaternary system may display one-, two-, three-, or four-mode behavior in the optic-phonon modes, and show transitions between these types of behavior as the alloy system is explored along different compositional trajectories. These behaviors are indeed more complicated than the one- or two-mode behaviors of the diatomic-pseudobinary systems. The ATA provides a convenient way to study the one-phonon density of states to either assign or possibly predict the behavior in a given system. Since the ATA formulation developed in this paper is based on a linear chain, other criteria must be invoked to eliminate spurious modes that arise from the neglect of well-known three-dimensional effects, e.g., as has been done in Ref. 7.

ACKNOWLEDGMENTS

The authors wish to acknowledge many interesting discussions with Dr. R. M. Martin, Dr. T. M. Hayes, and Dr. D. Chadi. We are indebted to Professor G. L. Pearson of Stanford University for the loan on a $Ga_{1-x}Al_xAs$ sample. Finally, we wish to thank R. D. Burnham for growing the $Ga_{1-x}Al_xP$ crystal.

[1]G. Lucovsky, R. D. Burnham, A. S. Alimonda, and H. A. Six, in *Proceedings of the Twelfth International Conference on the Physics of Semiconductors*, edited by M. H. Pilkuhn (B. G. Teuber, Stuttgart, 1974), p. 326.
[2]H. W. Verleur and A. S. Barker, Phys. Rev. 149, 715 (1966).
[3]Y. S. Chen, W. Shockley and G. L. Pearson, Phys. Rev. 151, 648 (1966).
[4]E. Ilegems and G. L. Pearson, Phys. Rev. B 1, 1576 (1970).
[5]G. Lucovsky, M. H. Brodsky, and E. Burstein, in *Proceedings of the International Conference on Localized Excitations in Solids*, edited by R. F. Wallis (Plenum, New York, 1968), p. 592.
[6]I. F. Chang and S. S. Mitra, Adv. Phys. 20, 359 (1971).
[7]G. Lucovsky, M. H. Brodsky, and E. Burstein, Phys. Rev. B 2, 3295 (1970).
[8]P. Mazur, E. W. Montroll, and R. B. Potts, J. Wash. Acad. Sci. 46, 2 (1956).
[9]P. N. Sen and W. M. Hartmann, Phys. Rev. B 9, 367 (1974).
[10]L. Schwartz, F. Brouers, A. V. Vedyayeran, and H. Ehrenreich, Phys. Rev. B 4, 3383 (1971).
[11]B. Velický, S. Kirkpatrick, and H. Ehrenriech, Phys. Rev. 175, 747 (1968).
[12]W. A. Kamitakahara and D. W. Taylor, Phys. Rev. B 10, 1190 (1974).
[13]N. D. Strahm and A. L. McWorter, in *Light Scattering Spectra of Solids*, edited by G. B. Wright (Springer-Verlag, New York, 1969), p. 455.
[14]G. Lucovsky, M. H. Brodsky, M. F. Chen, R. J. Chicotka, and A. T. Ward, Phys. Rev. B 4, 1945 (1971).
[15]J. L. Varnell, J. L. Warren, R. G. Wenzel, and P. J. Dean in *Neutron Inelastic Scattering* (International Atomic Energy Agency, Vienna, 1968), p. 301.
[16]G. Lucovsky, R. D. Burnham, and P. N. Sen, Bull. Am. Phys. Soc. 20, 1974.
[17]D. W. Taylor, Phys. Rev. 156, 1617 (1967).
[18]T. Kaplan and M. Mostoker, Phys. Rev. B 9, 1783 (1974).
[19]P. Dean, Rev. Mod. Phys. 44, 127 (1972).